frontiers | Frontiers in Earth Science

TYPE Original Research
PUBLISHED 19 September 2025
DOI 10.3389/feart.2025.1650751

OPEN ACCESS

EDITED BY
Tao Hu,
China University of Petroleum, Beijing, China

REVIEWED BY
Shuai Yin,
Xi'an Shiyou University, China
Yuqi Wu,
China University of Petroleum, Beijing, China
Kong Deng,
China University of Geosciences, China

*CORRESPONDENCE
Peng Jin-ning,
pengjn.syky@sinopec.com

RECEIVED 20 June 2025
ACCEPTED 18 August 2025
PUBLISHED 19 September 2025

CITATION
Jin-Ning P, Chongjiao D, Longlong L and Mingzhe D (2025) Occurrence and recoverability of shale oil in Paleogene formation, Subei Basin.
Front. Earth Sci. 13:1650751.
doi: 10.3389/feart.2025.1650751

Occurrence and recoverability of shale oil in Paleogene formation, Subei Basin

Peng Jin-Ning*, Du Chongjiao, Li Longlong and Deng Mingzhe

Wuxi Petroleum Geology Research Institute, SINOPEC Exploration & Production Research Institute, Wuxi, Jiangsu, China

In recent years, significant breakthroughs have been made in the exploration and development of lacustrine shale oil, but the stable and guaranteed production of shale oil still faces huge challenges. Quantitative characterization of the occurrence state of shale oil and accurate evaluation of the movable oil content are the key scientific issues that need to be solved for the efficient exploration and development of lacustrine shale oil. The second and fourth sections of the Funing Formation in the northern Jiangsu Basin are preferred layers for the exploration and development of continental shale oil in eastern China. However, there are few reports on the occurrence status and availability of shale oil in these areas. This study systematically investigates the oil-bearing characteristics and mobility mechanisms of shale and interlayer systems in the second and fourth membersof the Funing Formation (E_1f_2, E_1f_4), Subei Basin, through an integrated approach combining multi-temperature pyrolysis, nuclear magnetic resonance (NMR) analysis, and limited production data from 23 wells. Key findings reveal:1) Shale matrices exhibit low total retained oil content (<5.0 mg/g), dominated by adsorption-miscible oil (40%–95% of total hydrocarbons), with its proportion inversely correlated to burial depth (R^2 = 0.78). Light free oil content remains exceptionally low (<0.1 mg/g), yielding a mobility ratio <3%. In contrast, interlayers and adjacent sandstones demonstrate significantly higher oil saturation (>5 mg/g), predominantly as free-phase oil (60%–82%), with light free oil exceeding 0.25 mg/g and mobility ratios of 4–7%—comparable to pre-stimulation Bakken tight sandstones (5%); 2) NMR-derived T_2 cutoff values (6 m) and throat radius thresholds (>0.18 μm) indicate movable shale oil primarily resides in fracture networks (contributing 68%–85% of permeability) and secondary micropores. Phase-state analysis reveals free oil > adsorbed oil within these conductive pathways, corroborated by production data from fractured carbonate reservoirs.3) Fractured lacustrine carbonates exhibit high initial yields (e.g., Well XuX38: 15.8 t/d) but rapid decline rates (68% within 90 days). Conversely, intra-source interlayer systems demonstrate sustained production (Well TianX96: <15% decline over 18 months), attributed to stable pressure maintenance and effective matrix-fracture connectivity. Economic analysis suggests 2.1× higher EUR (Estimated Ultimate Recovery) in interlayer systems compared to fractured carbonates.

KEYWORDS

funing formation, Subei Basin, shale oil, occurrence state, recoverability

1 Introduction

Shale oil, as an important component of unconventional oil and gas resources, has become a new focus in unconventional exploration in recent years (Sonnenberg and Pramudito, 2009; U.S. Energy Information Administration, 2016; Jia et al., 2012; Zou et al., 2015; Yang et al., 2013; Cui et al., 2022; Guo et al., 2023; Hu et al., 2024). In 2022, the United States emerged as the resource-producing country with the highest growth in global crude oil production, with tight oil—primarily shale oil—contributing the most, increasing by 275.0786 million tons year-on-year (Wang et al., 2023). In China, continental shale oil has achieved industrial breakthroughs in multiple basins, including the Junggar, Ordos, Bohai Bay, Songliao, Sichuan, and Subei basins (Wu et al., 2022; Jiang et al., 2023b; Jiang et al., 2023c; Wang et al., 2022; Feng, 2022; Yun et al., 2023; Jiang et al., 2023a; Wu et al., 2024; Wu et al., 2025a; Wu et al., 2025b).

The second and fourth members of the Funing Formation in the Subei Basin are the principal source rocks for conventional oil and gas, and they also constitute the primary target intervals for the formation of unconventional shale oil reservoirs (Liu et al., 2014; Qiu et al., 2005). According to several scholars and experts, the shale oil resources within the Funing Formation could be the most promising replacement for conventional resources in the Subei Basin (Zheng and Peng, 2013; Wang et al., 2016). With ongoing research and exploration into shale oil, earlier studies have made significant advances in understanding the formation conditions, reservoir characteristics, fracture prediction, and enrichment patterns of these shale systems (Wang and Duan, 2016; Wang et al., 2016; Zhang et al., 2004; Zan et al., 2016). However, there is still a relative lack of research regarding the occurrence states and mobility of shale oil within the Funing Formation. Accurately evaluating how shale oil exists within reservoirs—its forms, states, and recoverability—is currently a key bottleneck in shale oil exploration and one of the urgent issues that needs to be resolved (Yan et al., 2017; Xiong et al., 2017). This paper is based on a systematic analysis of shale, interlayers, and adjacent carbonate and sandstone units from the second and fourth members of the Funing Formation. By employing multi-step pyrolysis and nuclear magnetic resonance (NMR) techniques, the study aims to investigate and evaluate the oil-bearing properties, occurrence states, and mobility of shale oil in both intra-source interlayers and adjacent rocks (including the first and third members of the formation), with the goal of providing insights into the exploration and development of shale oil in the Subei Basin.

2 Regional geological overview

The Subei (Northern Jiangsu) Late Cretaceous-Cenozoic Basin overlies the Mesozoic basins of the Lower Yangtze region, with its internal structural units controlled by the Indosinian-Yanshanian tectonic framework (Wang et al., 2012; Zhang et al., 2010; Wang et al., 2016). Based on the relationship between the Subei Basin and surrounding regional structural units, its interior can be divided into four second-order structural units: the Dongtai Depression, Jianhu Uplift, Yanfu Depression, and Binhai Uplift. Each depression can be further subdivided into several sub-level sags and low uplifts (Figure 1a). Among them, the four major sags within the Dongtai Depression—Jinhu, Gaoyou, Qintong, and Hai'an—are the key exploration areas for oil and gas discoveries.

Although the stratigraphy of the Funing Formation in the Subei Basin exhibits notable lithological and electrical property variations across different depressions, a general vertical rhythmic pattern of sandstone–mudstone–sandstone–mudstone is observed from the first to the fourth members. Member E_1f_1 and E_1f_3 are characterized by the development of large deltaic depositional systems, featuring widespread sandstone reservoirs, which predominantly consist of single sets of sandstone beds. Member E_1f_2 and E_1f_4, in contrast, are dominated by extensive lacustrine depositional systems, hosting widely distributed source rocks primarily composed of dark gray mudstone and shale. These members also contain thin carbonate and tight sandstone interlayers embedded within the shale source rocks. Overall, these lithological features provide the material foundation necessary for the formation of shale oil. Current research indicates that the Funing Formation in the Subei Basin comprises:Four regionally continuous and mature source rock intervals ($E_1f_2^1$, $E_1f_2^2$, $E_1f_2^3$, $E_1f_4^1$), Three tight sandstone reservoirs closely associated with source rocks ($E_1f_1^1$, $E_1f_2^3$ and $E_1f_3^3$), Three intra-source carbonate or sandstone interlayers ($E_1f_1^1$, $E_1f_2^3$ and $E_1f_3^3$), As well as two sets of regional interlayers ($E_1f_2^1$ caprock and $E_1f_4^2$), which serve as effective seals.

Considering that the source rocks of $E_1f_4^2$ and $E_1f_2^3$ (in the Gaoyou and Jinhu Sag) have low organic richness and poor hydrocarbon generation potential, and due to their considerable thickness, they act as vertical barriers to the overlying oil-prone layers and underlying tight reservoirs. Taking into account the lateral migration capacity of faults and sand bodies, five favorable shale oil accumulation models can be identified (Table 1; Figure 1b), including:1. Source-below model: where source rocks ($E_1f_2^2$) underlie tight sandstone reservoirs ($E_1f_1^1$), 2. Intra-source model: formed by source rocks ($E_1f_2^1$, $E_1f_2^2$, $E_1f_2^3$) and their internal carbonate or sandstone interbeds, 3. Distal-source fault–sandstone-guided model: involving source rocks in $E_1f_4^1$ and E_1f_2 and tight sandstone reservoirs in E_1f_2, E_1f_3, and E_1f_1 connected through faults and lateral migration pathways.

3 Samples and experimental methods

3.1 Sample collection

To investigate the occurrence states of shale oil in the Funing Formation under different lithological combinations, systematic sampling was conducted on shale, carbonate rock (tight sandstone) interbeds within source rocks, and adjacent tight sandstone layers in key sags (Gaoyou and Jinhu) of the study area. A total of 165 core samples and 213 cuttings samples were collected from 17 wells. Subsequent experimental analyses included multi-temperature step pyrolysis on 60 samples, organic carbon testing on 170 samples, and nuclear magnetic resonance (NMR) analysis on 174 samples.2.2 Experimental Test Methods.

3.1.1 Organic carbon

The total organic carbon content of the core samples was determined using the LECO CS-230 carbon analyzer of China

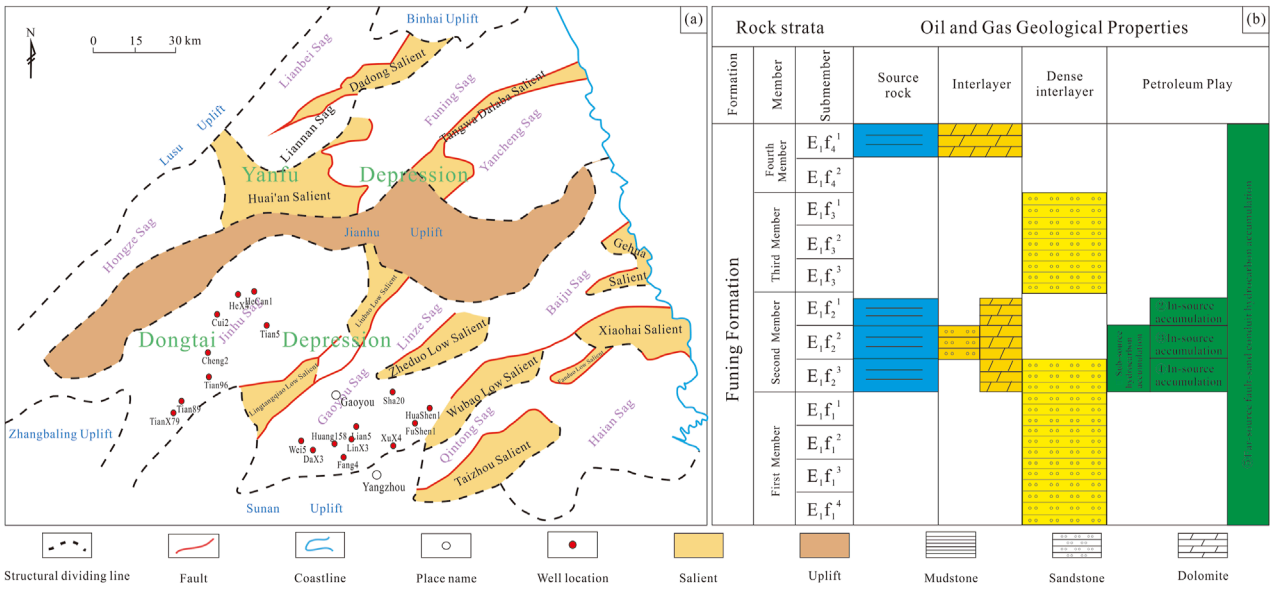

FIGURE 1
Tectonic zoning map and the columnar diagram of the strata in the northern Jiangsu Basin. **(a)** is the structural zoning map of the basin in northern Jiangsu. **(b)** is the distribution of tight oil accumulation assemblage in Funing Formation, Subei Basin.

University of Petroleum (Beijing). To remove inorganic carbon, the core samples were crushed and sieved through an 80-mesh sieve, and then reacted with a 10% (volume fraction) HCL solution for more than 2 h until the reaction was complete. The measurement accuracy is estimated to be 0.45% of the measured value.

3.1.2 Multi-temperature pyrolysis

This study obtained the occurrence state of shale oil in the samples through multi-temperature pyrolysis experiments. The experimental analysis was conducted using the improved Rock-Eval 6 pyrolysis instrument of Wuxi Petroleum Geology Research Institute of Sinopec Petroleum Exploration and Development Research Institute. $S_{1\text{-}1}$ (light oil component) was measured at a constant temperature of 200 °C for 1 min. Then, it was heated to 350 °C at a rate of 25 °C/min and kept at a constant temperature for 1 min to measure $S_{1\text{-}2}$ (light - medium oil component). Then, the temperature was raised to 450 °C at a rate of 25 °C/min and maintained at a constant temperature for 1 min to measure $S_{2\text{-}1}$ (heavy hydrocarbon and gelatinous asphaltene components). Finally, the temperature was raised to 600 °C at the same rate to measure $S_{2\text{-}1}$ (kerogen pyrolytic hydrocarbon).

3.1.3 NMR experiments

The two-dimensional nuclear magnetic resonance (NMR) experiments were conducted using an American Core Company MRCore-040V 23 MHz NMR instrument to quantitatively measure the longitudinal relaxation time (T_1) and transverse relaxation time (T_2) of ^{1}H-containing compounds in shale samples under conventional processing conditions, with a total of 5 samples analyzed.

For the organic matter extraction experiments, dichloromethane (DCM) solvent was employed in a Soxhlet extraction apparatus to isolate solvent-soluble components from the samples. The extraction process was carried out at 70 °C for 48 h to quantify the retained oil within the shale samples. Following the extraction experiments, the two-dimensional NMR measurements were repeated.

4 Occurrence state of shale oil

4.1 Composition characteristics of shale oil

During the room-temperature storage of shale, a significant portion of the light hydrocarbon components (C_6–C_{13}) in the samples is lost. These lost light hydrocarbons constitute an important part of the free oil in shale oil. Directly using pyrolysis parameters to represent residual hydrocarbons often underestimates the actual free oil content. Therefore, light hydrocarbon correction is necessary to restore the lost light hydrocarbons before pyrolysis experiments, thereby accurately characterizing the occurrence state of shale oil.

A comparative analysis was conducted between the pyrolysis parameter S_1 of freeze-preserved samples and the pyrolysis parameter S_1' of samples stored at room temperature to calculate the light hydrocarbon correction factor ($K = S_1/S_1'$) (Gong et al., 2024). Due to the excessive number of data points, it was difficult to fit a curve. Instead, the samples were sorted by depth, and averages were taken every 10 m to establish a chart showing the variation of the light hydrocarbon correction factor for shale oil with depth (see Figure 2). The light hydrocarbon correction factor mainly ranges from 1.1 to 4.2, with an average of 2.6. As shown in Figure 2, the correction factor increases with depth, reflecting a trend of higher organic matter maturity and a significant increase in the proportion of light hydrocarbons as depth increases.

The total quantity of retained oil in various occurrence states within shale or sandstone serves as a critical indicator of oil-bearing potential. Two primary methods—solvent extraction

TABLE 1 Distribution of source - reservoir superimposed relationship and accumulation association in E_1f, Subei Basin.

Stratum		Reservoir layer			Oil generation layer		Oil and gas geological properties			Develop layers, regions and lithology	
Member	Submember	Thickness/m	Φ %	K mD	Thickness/m	TOC %	Sub-source	In-source	Far-source		
E_1f_4	$E_1f_4^1$				>100	1.2			⑤ Far-source fault-sand conduit hydrocarbon accumulation	Dense sandstone of Gaoyou Sag	
	$E_1f_4^2$				>100	0.74					
E_1f_3	$E_1f_3^1$	<30	8–12	0.1–1							
	$E_1f_3^2$										
	$E_1f_3^3$	<20									
										Laminar carbonate rocks	Biological limestone and sandstone interlayers in the Jinhu and Gaoyou Sag
E_1f_2	$E_1f_2^1$	5–10	3.2		40–80	2.14		② In-source			
	$E_1f_2^2$	5–10	8–26	2.2–79.8	60–80	1.29	① Sub-source	③ In-source			
	$E_1f_2^3$				5–10	0.98		④ In-source			
		<40	8–12	0.1–1							
E_1f_1	$E_1f_1^1$	<80	8–12	0.1–1						Dense sandstone of Gaoyou Sag	

10.3389/feart.2025.1650751

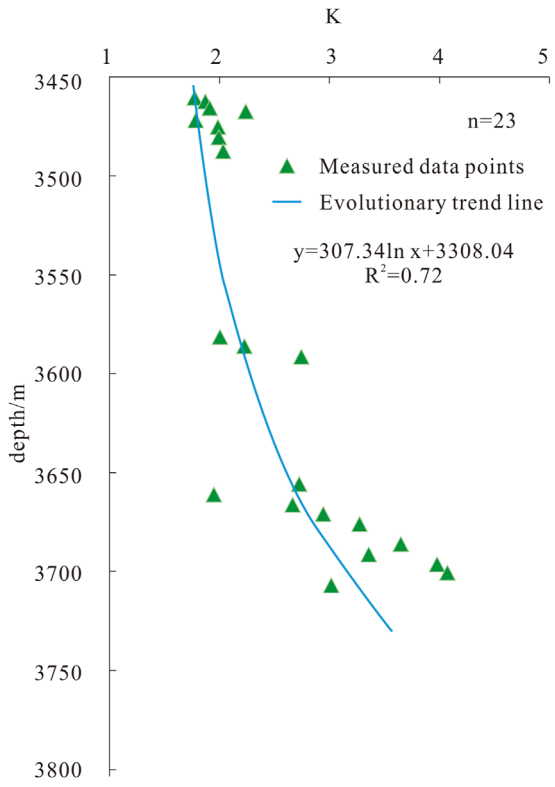

FIGURE 2
Relationship between light hydrocarbon correction factor (K) and depth for shale in the Funing Formation of the study area.

and thermal desorption—are commonly used for quantitatively analyzing retained oils in free and adsorbed states (Lang et al., 1996; Jiang et al., 2016). In this study, systematic analyses were conducted using multi-step pyrolysis on samples from the Funing Formation, including shale, intra-source carbonate (tight sandstone) interbeds, and adjacent tight sandstones (Table 2). The results were used to evaluate the oil-bearing characteristics and oil mobility in shale, interbeds, and neighboring tight sandstones. Among them, the pyrolytic hydrocarbon $S_{1\text{-}1}$ is primarily composed of light oil components existing in a free state, representing the most readily mobilizable oil currently available. $S_{1\text{-}2}$ mainly consists of light-medium oil components and also occurs in a free state. $S_{2\text{-}1}$ is dominated by heavy oil, resin-asphaltene components, coexisting with organic matter in an adsorbed-dissolved state. $S_{2\text{-}2}$ primarily originates from regenerated hydrocarbons through kerogen pyrolysis in shale. Therefore, the total free hydrocarbon content is the sum of $S_{1\text{-}1}$ and $S_{1\text{-}2}$, while the total retained oil volume comprises both free hydrocarbons and adsorbed-dissolved oil, serving as critical parameters for characterizing oil-bearing properties.

Based on the analysis of shale samples from the E2 and E4 Members in the Gaoyou and Jinhu Sags (the main exploration areas of the Subei Basin), along with their interlayers and adjacent tight sandstone layers (Table 2; Figures 3a, b), the total retained oil volume in the E2 and E4 shale of the Jinhu Sag is generally less than 5.0 mg/g, with some samples below 0.5 mg/g (Figure 3a). Adsorbed-dissolved oil dominates the retained oil, accounting for 40%–95% of the total. The proportion of adsorbed-dissolved oil exhibits a decreasing trend with increasing burial depth. Light free oil content remains extremely low (<0.1 mg/g), and the current mobilizable oil ratio is below 2%. In contrast, the total retained oil volume in interbedded shales and adjacent oil-bearing tight sandstones of the E2 and E4 Members typically exceeds 5 mg/g (maximum 14.02 mg/g), with free oil as the dominant phase. Light free oil content generally surpasses 0.25 mg/g, yielding a current mobilizable oil ratio of 4%–7%. This aligns closely with the ~5% recovery rate observed in unstimulated Middle Bakken tight sandstone intervals in North America (Liu et al., 2016).

In the E2 and E4 shale of the Gaoyou Sag, the total retained oil volume generally remains below 5.0 mg/g, with some samples registering less than 0.5 mg/g. Adsorbed-dissolved oil predominates, accounting for 50%–92% of the total retained oil. This proportion exhibitis a decreasing trend with increasing burial depth. Light free oil content is consistently low (<0.2 mg/g), resulting in a current mobilizable oil ratio below 3%. Conversely, interbedded shales and adjacent oil-bearing tight sandstones within the E2 and E4 Members typically contain retained oil volumes exceeding 15 mg/g (Figure 3b), dominated by free oil. Light free oil content in these intervals generally surpasses 0.50 mg/g, yielding a current mobilizable oil ratio of 3%–4%.

As shown in Figure 4 illustrating the relationships between free oil ($S_{1\text{-}1}$, $S_{1\text{-}2}$), adsorbed-dissolved oil ($S_{2\text{-}1}$), and TOC, free oil primarily resides in inorganic pore-fracture systems (Figure 4a,b), whereas adsorbed-dissolved oil predominantly occurs within Figure 4c organic matter, demonstrating a moderate positive correlation with TOC (Figure 4c).

4.2 Shale oil saturation characteristics

Experience from North American shale oil exploration shows that productive intervals—whether mudstone or sandstone—typically exhibit an oil saturation index ($S_1 \times 100$/TOC) greater than 100 (Wang, 2013). Statistical results from pyrolysis analyses of E_1f_2 and E_1f_4 samples from the main shale oil sags in Gaoyou and Jinhu indicate (Figure 5): The E_1f_2 section is generally moderately to highly oil-bearing, with some samples showing an oil saturation index >100, signifying shale oil potential (Figure 5a). The E_1f_4 section is mostly low in oil content, with only a few samples indicating shale oil potential (Figure 5b). The data suggest that the E_1f_2 mudstone–shale system has good exploration potential, and that the oil saturation index tends to increase with thermal maturity (Tmax).

5 Shale oil mobility

5.1 NMR characteristics of shale oil mobility

Mobility and movable fluid content are critical parameters for shale oil evaluation. Zhou et al. (2014) applied nuclear magnetic resonance (NMR) technology to analyze movable fluids in shale gas reservoirs, tight sandstone, and tight limestone

TABLE 2 Evaluation of oily and mobility in shale, interlayer and adjacent sandstone in E_1f_2 and E_1f_4 in key sag, Subei Basin.

Lithology	Well number	Stratum	Sample position	Free light oil S'_{1-1} (mg/g)	Free medium - heavy oil S'_{1-2} (mg/g)	Adsorb miscible oils S'_{2-1} (mg/g)	Total free oil content (mg/g)	Total retained oil volume (mg/g)	Free hydrocarbons S′1-2/Total retained oil (%)	Adsorption - miscible oil/Total retained oil (%)	Free hydrocarbons S′1-1/Total retained oil (%)	Pyrolysis regenerated oil S′2-2 (mg/g)	Sag
Light grey siltstone	Cheng2	E_1f_2	interlayer	0.07	2.46	1.02	2.53	3.55	69.30	28.73	1.97	0.50	Jinhu
Grey silty mudstone	Cheng2	E_1f_2	interlayer	0.00	0.01	0.02	0.01	0.03	33.33	66.67	0.00	0.05	
Light grey calcareous mudstone	Cui2	E_1f_3	interlayer	0.00	0.15	1.84	0.15	1.99	7.54	92.46	0.00	2.73	
Grey siltstone	Dai1	E_1f_2	interlayer	0.01	1.18	7.59	1.19	8.78	13.44	86.45	0.11	7.22	
Dark grey marl	HeX4	E_1f_4	Adjacent layer	0.00	0.12	2.03	0.12	2.15	5.58	94.42	0.00	4.32	
Grey siltstone	HeX4	E_1f_2	interlayer	0.41	6.11	3.25	6.52	9.77	62.54	33.27	4.20	1.55	
Dark grey mudstone	HeX4	E_1f_2	Shale	0.00	0.01	0.02	0.01	0.03	33.33	66.67	0.00	0.02	
Grayish-black mudstone	HeCan1	E_1f_2	Shale	0.02	0.98	1.29	1.00	2.29	42.79	56.33	0.87	2.52	
Grayish-black mudstone	HeCan 1	E_1f_2	Shale	0.06	1.33	3.07	1.39	4.46	29.82	68.83	1.35	4.96	
Grayish-black mudstone	HeCan 1	E_1f_2	Shale	0.00	0.01	0.04	0.01	0.05	20.00	80.00	0.00	0.08	
Grey siltstone	Tang5	E_1f_2	interlayer	0.61	8.31	5.10	8.92	14.02	59.27	36.38	4.35	3.07	

(Continued on the following page)

10.3389/feart.2025.1650751

TABLE 2 (*Continued*) Evaluation of oily and mobility in shale, interlayer and adjacent sandstone in E_1f_2 and E_1f_4 in key sag, Subei Basin.

Lithology	Well number	Stratum	Sample position	Free light oil S'_{1-1} (mg/g)	Free medium - heavy oil S'_{1-2} (mg/g)	Adsorb miscible oils S'_{2-1} (mg/g)	Total free oil content (mg/g)	Total retained oil volume (mg/g)	Free hydrocarbons S′1-2/Total retained oil (%)	Adsorption - miscible oil/Total retained oil (%)	Free hydrocarbons S′1-1/Total retained oil (%)	Pyrolysis regenerated oil S′2-2 (mg/g)	Sag
Dark grey sandy mudstone	Tian89	E_1f_2	interlayer	0.00	0.19	0.35	0.19	0.54	35.19	64.81	0.00	0.39	
Grey sandstone	TianX79	E_1f_4	interlayer	0.51	6.29	2.97	6.80	9.77	64.38	30.40	5.22	2.51	
Dark grey mudstone	TianX79	E_1f_4	Shale	0.00	0.03	0.06	0.03	0.09	33.33	66.67	0.00	0.10	
Grey mudstone	DaX3	E_1f_2	Mud shale	0.00	0.65	5.52	0.65	6.17	10.53	89.47	0.00	7.99	Gaoyou
Grey mudstone	Fang4	E_1f_3	Adjacent layer	0.21	3.56	7.58	3.77	11.35	31.37	66.78	1.85	13.90	
Grayish-black mudstone	FuShen1	E_1f_1	Adjacent layer	0.02	0.34	0.33	0.36	0.69	49.28	47.83	2.90	0.29	
Grayish-black mudstone	FuShen 1	E_1f_2	Mud shale	0.07	0.92	1.10	0.99	2.09	44.02	52.63	3.35	1.96	
Grayish-black mudstone	FuShen 1	E_1f_4	Mud shale	0.02	0.77	3.29	0.79	4.08	18.87	80.64	0.49	9.21	
Dark grey mudstone	HuaShen 1	E_1f_3		0.02	0.14	0.12	0.16	0.28	50.00	42.86	7.14	0.59	
Grey siltstone	Lian5	E_1f_2	interlayer	0.00	0.02	0.01	0.02	0.03	66.67	33.33	0.00	0.01	
Dark grey marl	Lian 5	E_1f_3	Adjacent layer	0.00	0.05	0.23	0.05	0.28	17.86	82.14	0.00	0.56	

(Continued on the following page)

10.3389/feart.2025.1650751

TABLE 2 (*Continued*) Evaluation of oily and mobility in shale, interlayer and adjacent sandstone in E_1f_2 and E_1f_4 in key sag, Subei Basin.

Lithology	Well number	Stratum	Sample position	Free light oil S'_{1-1} (mg/g)	Free medium - heavy oil S'_{1-2} (mg/g)	Adsorb miscible oils S'_{2-1} (mg/g)	Total free oil content (mg/g)	Total retained oil volume (mg/g)	Free hydrocarbons S′1-2/Total retained oil (%)	Adsorption - miscible oil/Total retained oil (%)	Free hydrocarbons S′1-1/Total retained oil (%)	Pyrolysis regenerated oil S′2-2 (mg/g)	Sag
Black mudstone	Lian 5	E_1f_4	Mud shale	0.00	0.02	0.09	0.02	0.11	18.18	81.82	0.00	0.16	
Grayish-black mudstone	LinX3	E_1f_2	Mud shale	0.00	0.04	0.18	0.04	0.22	18.18	81.82	0.00	0.24	
Grayish-white sandstone	Sha20	E_1f_1	Adjacent layer	0.86	14.49	5.57	15.35	20.92	69.26	26.63	4.11	2.73	
Dark grey sandstone	Sha20	E_1f_1	Adjacent layer	0.72	12.90	6.02	13.62	19.64	65.68	30.65	3.67	2.82	
Dark grey siltstone	Wei5	E_1f_1	Adjacent layer	0.59	9.43	7.69	10.02	17.71	53.25	43.42	3.33	4.50	

10.3389/feart.2025.1650751

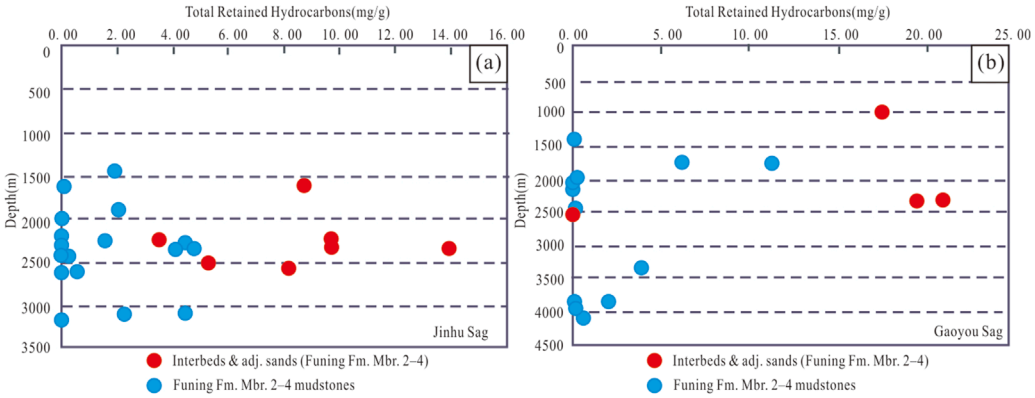

FIGURE 3
Total hydrocarbon retention in shale, interlayer and adjacent sandstones in second and fourth members of Funing Formation, Jinhu and Gaoyou sags, Subei Basin, Red dots indicate interbeds and adjacent sands, while blue dots represent Funing Formation member two to four mudstones. **(a)** The total amount of retained oil in the Fuer and Fusi sections of the Zhongjinhu Depression is less than 5.0mg/g, and the total amount of retained oil in the interlayer of the shale and the adjacent sandstone (with oil content) is generally more than 5 mg/g. **(b)** The total amount of retained oil in the shale of the Fuer and Fusi sections in the Zhonggaoyou Depression is generally less than 5.0mg/g, and in some samples, it is less than 0.5 mg/g. The total amount of retained oil in the interlayer of shale and the adjacent sandstone (with oil content) is generally greater than 15 mg/g.

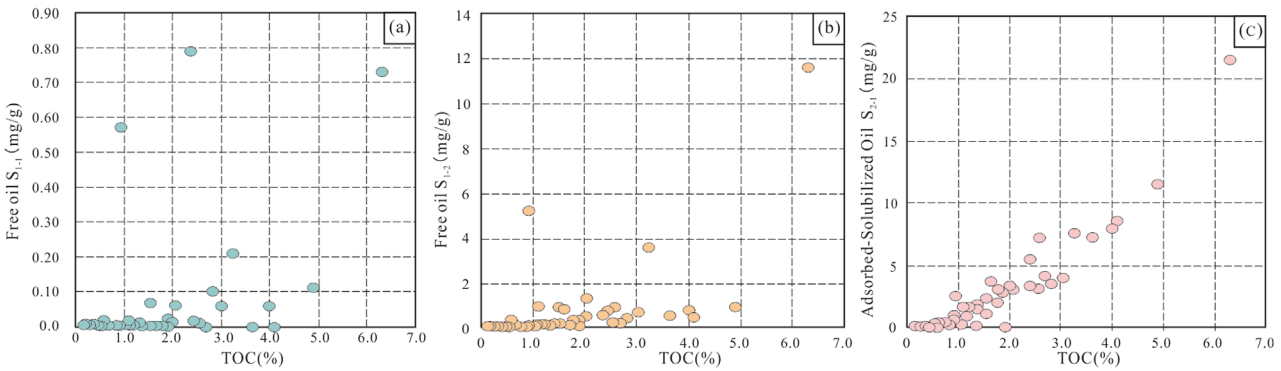

FIGURE 4
TOC content vs. tight oil components of Funing Formation, Subei Basin. **(a)** shows Free oil S_{1-1} vs. TOC, **(b)** shows Free oil S_{1-2} vs. TOC, and **(c)** shows Adsorbed-Solubilized Oil S_{2-1} vs. TOC.

reservoirs. Zhang et al. (2014) combined experimental analysis with well-logging data to investigate shale oil mobility through systematic studies of shale porosity, compressibility, rock mechanical properties, oil saturation, gas-oil ratio, and crude oil saturation pressure. This study primarily utilizes NMR data from 174 E_1f_4 shale samples of Well Huang 158 to analyze the mobility and occurrence state of shale oil in the E_1f lacustrine carbonate-rich shales of the Subei Basin. The NMR results reveal that most shale samples exhibit unimodal T_2 spectra (Figure 6), indicating no detectable movable fluids. Only 62 samples show bimodal or trimodal T_2 spectra, suggesting the presence of limited movable fluids. The movable fluid content in these samples is generally <20.68% (average 6.11%; Table 3), with a T_2 cutoff time of 6 m (corresponding to a pore-throat radius of 0.18 μm). These findings imply that:Pore-throat radii in E_1f_4 shales are predominantly <0.18 μm.Movable fluids (interpreted as crude oil based on fracturing and production testing) are only retained in micropores with radii >0.18 μm within a limited subset of shales.

However, the linear relationship between the content of movable fluid in the E_1f_4 shale of Well Huang 158 and its matrix porosity (Figure 7a) and organic matter abundance (Figure 7b) is not obvious, reflecting that movable shale oil should mainly occur in fractures, that is, structural fractures are the main occurrence space of movable shale oil, and some micropores (with a roar radius greater than 0.18 μm) are secondary occurrence Spaces. This determines that the occurrence phase state of shale oil should mainly be the free state, followed by the adsorbed state.

5.2 Production test characteristics of shale oil mobility

This study takes well locations Xu X38 and Tian 96 as examples to elaborate on the characteristics of shale oil mobility test production in two different types of shale reservoirs: intra-source fractured type and intra-source interlayer type. The burial depth of

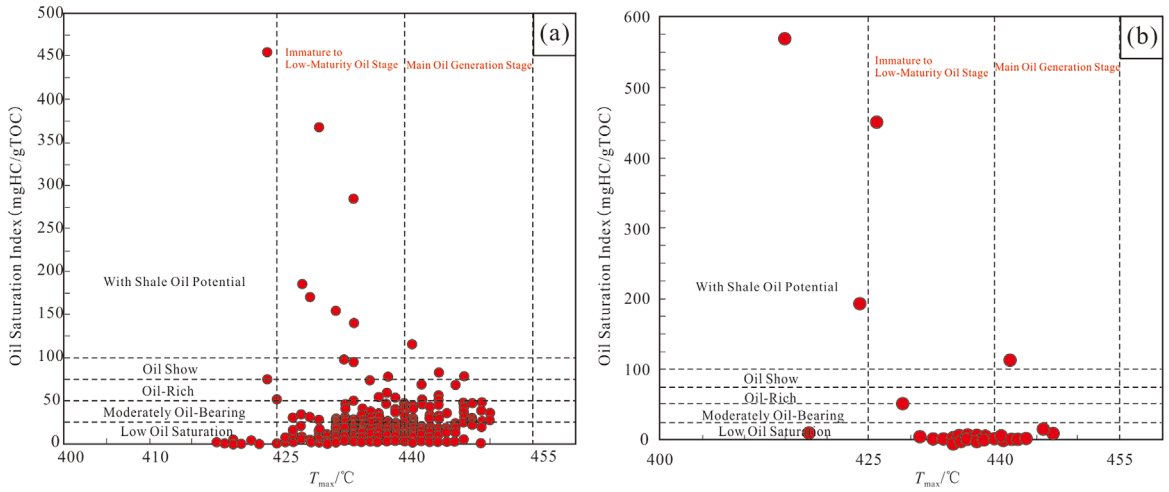

FIGURE 5
Relationship between oil saturation index and T_{max} of second and fourth members of Funing Formation, Subei Basin. Both graphs use red data points and vertical dotted lines to indicate the transition from the immature stage to the main oil-producing stage. The horizontal dotted line classifies the oil saturation as low oil content, medium oil content, rich oil content or oil content. **(a)** The strata in the Fuer section of the northern Jiangsu Basin are mainly of medium to high oil content, and **(b)** the strata in the Fuer section of the northern Jiangsu Basin are mainly of low oil content.

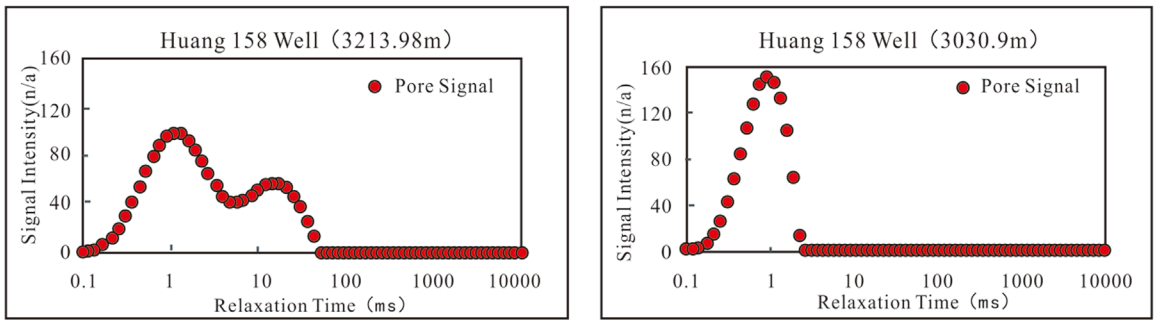

FIGURE 6
T_2 distribution spectrum by NMR analysis of lamillar lacustrine carbonate, Subei Basin.

TABLE 3 Movable fluid content in shales in E_1f_4, well Huang158.

Crack development	Movable fluid,%		Φ,%
	All samples	There are movable fluid samples	All samples
Developmental crack	0.17 (17)	0.14~2.52/1.47 (2)	0.24~6.58/2.10 (17)
Multiple development cracks	3.34 (89)	0.01~20.68/6.75 (44)	0.26~13.2/4.20 (89)
Thin-layered, 2 page-shaped	0.27 (32)	1.06~3.80/2.15 (4)	1.5~10.18/6.00 (32)
Thin-layered, developed cracks	0.81 (36)	0.14~11.58/4.86 (6)	1.39~10.36/6.20 (36)

the Xu X38 E_1f_2 shale oil reservoir ranges from 2580 m to 2840 m, and the oil-bearing layers are E_1f_2 page 2 (3,019.3m–3021.3 m) and E_1f_2 page 3 (3,076.3m–3077.6 m). According to the drilling data of Well Xu X38, the lithology of the upper oil-bearing layer is mainly dark gray massive grey mudstone, with underdeveloped margins but rich in biological debris. The lower oil-bearing layer is a stratified gray-bearing and cloud-bearing shale with well-developed margins and a thickness of 41 m. The average TOC of the upper oil-bearing layer is 2.80%. The average TOC of the lower oil-bearing layer is 1.39%, all of which have excellent oil generation capacity.

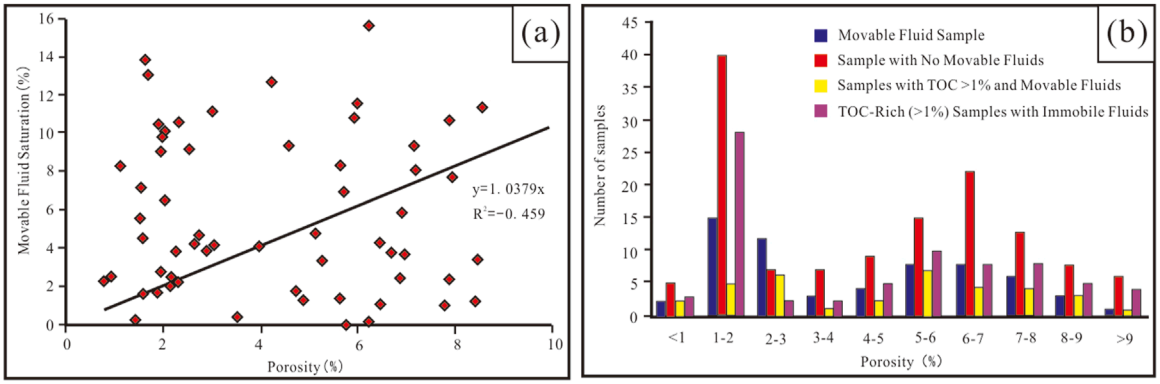

FIGURE 7
Relationship between movable fluid and matrix porosity, TOC content in fourth member of Funing Formation, well Huang 158, Gaoyou Sag, Subei Basin. **(a)** The relationship between the content of movable fluid in the E1f4 shale of Well Huang158 and its matrix porosity is not obvious. **(b)** the relationship between the content of movable fluid in the E1f4 shale of Well Huang158 and the abundance of organic matter is also not obvious, indicating that the movable tight oil should mainly exist in the fractures.

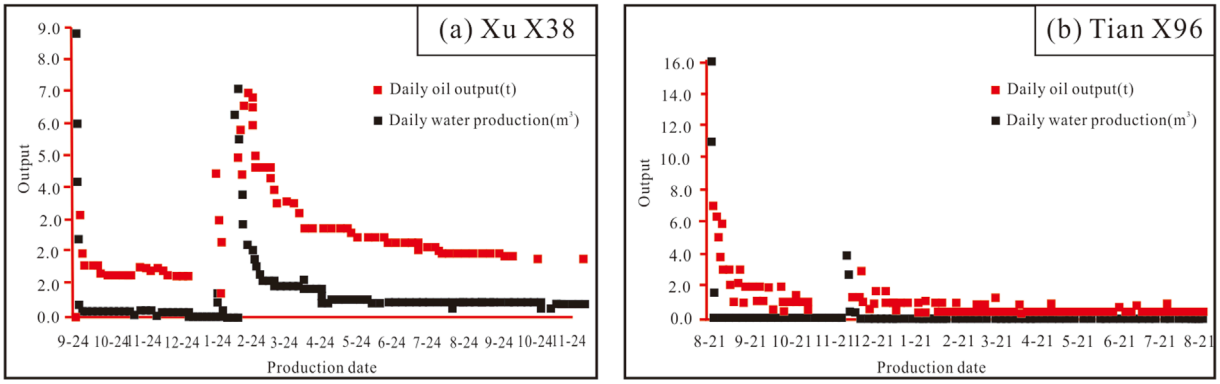

FIGURE 8
Production curves of tight oil in wells Xu X38 and Tian X96, Subei Basin. **(a)** Well Xu X38 indicates that although the initial output of fractured lacustrine carbonate tight oil is relatively high, the output decreases rapidly. **(b)** Well Tian X96 indicates that although the initial output of interlayer tight oil within the source is not high, the decline is slow.

Logging interpretation: The porosity of the reservoir ranged from 5.6% to 7.9%, with an average of 6.9%. Permeability: (0.2–6.6) $\times 10^{-3}$ μm^2, with an average of 1.1 × 10^{-3} μm^2; The oil saturation of the reservoir is 65.8%. In addition, the sensing resistivity of the oil-bearing layer is lower than that of the upper and lower surrounding rocks. The resistivity is in the shape of a "V" or a sharp knife, and the cracks are well developed. Well logging interpretation: There are multiple fracture development sections in Well X38 E_1f_2. During the fracture development sections, the oil and gas are active, with the highest peak of total hydrocarbons reaching 65.8% and 99.9% respectively. It belongs to the intra-source fracture type shale oil reservoir.

The oil-bearing strata of the Tian96 E_1f_2 shale oil reservoir include the sandstone interlayer within the $E_1f_2^1$ source and the sand body of the Xiatan dam in the $E_1f_2^2$ source. In the Tongcheng area where the oil reservoir is located, $E_1f_2^1$ is a subfacies deposition of shallow lakeside. Within the thick dark mudstone layer, thin-layer beach dam sand bodies are developed. The percentage content of sandstone is about 20%. The maximum single-layer thickness is 6.1 m and the minimum is 2 m. The rock types are feldspar siltstone and fine sandstone. The porosity ranges from 4.61% to 13.25%, with an average of 9.30%. The permeability was (0.10–7.37) $\times 10^{-3}$ μm^2, with an average of 3.51 × 10^{-3} μm^2. The oil saturation ranged from 14.28% to 32.19%, with an average of 23.24%. The lithology of the source rocks is mainly grayish-black striated marl, with some areas being striated to thin marl. Fossils of ostracods can be found in the striated marl, which is 19 m thick. The average TOC of shale was 2.51%, the average "A" of chloroform asphalt was 0.26%, and the average S_1 of pyrolyzed hydrocarbons was 0.44 mg/g. It belongs to the intra-source interlayer type shale oil reservoir.

From the perspective of the later oil test and production results of shale oil, although the initial output of fractured lacustrine carbonate shale oil is relatively high, the output decreases rapidly (Figure 8a), the production cycle is short, and the economic recoverability is limited. In contrast, although the initial output of the intra-source

interlayer shale oil is not high, it decreases slowly (Figure 8b), has a long production cycle, and has better economic recoverability.

6 Conclusion

1. The occurrence state and mobility of shale oil in the Funing Formation of the Subei Basin are jointly controlled by organic matter abundance, type, and porosity-permeability characteristics. Research indicates a significant positive correlation between organic matter abundance (TOC) and adsorbed-miscible oil, suggesting that high-TOC intervals are more conducive to oil adsorption and enrichment. In contrast, free oil primarily occurs in inorganic pore-fracture systems and shows a weaker relationship with TOC. Increasing organic matter maturity promotes the generation of light free oil, but the overall movable oil ratio remains relatively low. Nuclear magnetic resonance (NMR) analysis reveals that micropores with throat radii >0.18 μm serve as secondary storage spaces for movable fluids, while fracture systems act as the primary flow channels.
2. In the E_1f_2 and E_1f_4 mudstone–shale members, retained oil is dominated by adsorbed–miscible oil with low mobility, suggesting limited shale oil exploration potential. However, interbeds (carbonate or sandstone) and adjacent tight sandstones are dominated by free oil, have relatively higher movable oil content, and thus possess greater exploration potential.
3. In contrast, the initial production of fractured shale oil reservoirs within the source is high, but the production decreases rapidly, the production cycle is short, and the economic recoverability is limited. The initial production of tight sandstone oil reservoirs in interlayers or adjacent layers within the source is relatively low, but the decline is slow and the production cycle is long. They have good economic recoverability, providing a basis for the selection of favorable exploration areas for shale oil in the northern Jiangsu Basin.

Data availability statement

The original contributions presented in the study are included in the article/supplementary material, further inquiries can be directed to the corresponding author.

Author contributions

PJ-N: Project administration, Methodology, Writing – original draft. DC: Writing – review and editing, Validation, Visualization. LL: Investigation, Conceptualization, Writing – review and editing. DM: Data curation, Investigation, Writing – review and editing

Funding

The author(s) declare that financial support was received for the research and/or publication of this article. This research was supported by the Integrated Project of the National Natural Science Foundation of China's Enterprise Innovation and Development Joint Fund, “Enrichment Mechanism and Three-dimensional Development Method of Shale Oil in Continental Fault Depression Lake Basins” (U24B6002), and the project of Sinopec Group, “Research on the Development Characteristics and Evolution of the Paleogene Funing Basin in Northern Jiangsu” (P14073).

Conflict of interest

The authors declare that the research was conducted in the absence of any commercial or financial relationships that could be construed as a potential conflict of interest.

Generative AI statement

The author(s) declare that no Generative AI was used in the creation of this manuscript.

Any alternative text (alt text) provided alongside figures in this article has been generated by Frontiers with the support of artificial intelligence and reasonable efforts have been made to ensure accuracy, including review by the authors wherever possible. If you identify any issues, please contact us.

Publisher’s note

References

Cui, J. W., Zhang, Z. Y., Liu, G. L., Zhang, Y., and Qi, Y. (2022). Breakthrough pressure anisotropy and intra-source migration model of crude oil in shale. *Mar. Petroleum Geol.* 135, 105433. doi:10.1016/j.marpetgeo.2021.105433

Feng, D. J. (2022). Geological characteristics and exploration direction of Continental shale gas in Jurassic daanzhai member, sichuan basin. *Petroleum Geol. and Exp.* 44 (2), 219–230. doi:10.11781/sysydz202202219

Gong, H. J., Jiang, Z. X., and Zhu, F. (2024). Quantitative characterization and control factors of shale oil occurrence state in the shale of member 2 of funing formation in the gaoyou Sag,Subei basin. *J. Northeast Petroleum Univ.* 48 (02), 142–143. doi:10.3969/j.issn.2095-4107.2024.02.005

Guo, X. S., Li, M. W., and Zhao, M. Y. (2023). Shale oil development and utilization and its role in energy industry. *Bull. Chin. Acad. Sci.* 38 (1). doi:10.16418/j.issn.1000-3045.20221027001

Hu, T., Jiang, F. J., Pang, X. Q., Liu, Y., Wu, G., Zhou, K., et al. (2024). Identification and evaluation of shale oil micro-migration and its petroleum geological significance. *Petroleum Explor. Dev.* 51 (01), 127–140. doi:10.1016/s1876-3804(24)60010-8

Jia, C. Z., Zou, C. N., and Li, J. Z. (2012). Assesment criteria,main types,basic features and resource prospects of the shale oil in China. *Acta Pet. Sin.* 33 (3), 333–350.

Jiang, Q. G., Li, M. W., and Qian, M. H. (2016). Quantitative characterization of shale oil in different occurrence states and its application. *Petroleum Geol. and Exp.* 38 (6), 842–599.

Jiang, F. J., Huo, L. N., Chen, D., Cao, L., Zhao, R., Li, Y., et al. (2023a). The controlling factors and prediction model of pore structure in global shale sediments based on random forest machine learning. *Earth-Science Rev.* 241, 104442. doi:10.1016/j.earscirev.2023.104442

Jiang, F. J., Jia, C. Z., Pang, X. Q., Jiang, L., Zhang, C., Ma, X., et al. (2023b). Upper Paleozoic total petroleum system and geological model of natural gas enrichment in ordos basin, NW China. *Petroleum Explor. Dev. Online* 50 (2), 281–292. doi:10.1016/s1876-3804(23)60387-8

Jiang, F. J., Hu, M. L., Hu, T., Lyu, J., Huang, L., Liu, C., et al. (2023c). Controlling factors and models of shale oil enrichment in Lower Permian fengcheng formation, mahu sag, junggar basin, NW China. *Petroleum Explor. Dev.* 50 (04), 812–825. doi:10.1016/s1876-3804(23)60430-6

Lang, D. S., Guo, S. S., and Ma, D. H. (1996). The correlation method of pyrolysis parameters to evaluate hydrocarbon-beating samples from reservoirs. *Mar. Orig. Pet. Geol.* 1 (1), 53–55.

Liu, S. L., Duan, H. L., and Zhang, Y. (2014). Analysis of oil and gas exploration potential in F2 M ember Continental shale of subei basin. *Offshore oil.* 34 (3), 27–33. doi:10.3969/j.issn.1008-2336.2014.03.027

Liu, X., An, F., and Chen, Q. H. (2016). Technical analysis of enhancing crude oil recovery in tight oil reservoirs: a case study of tight oil in the bakken formation. *Petroleum Geol. Dev. Daqing* 35 (06), 164–169. doi:10.3969/j.issn.1000-3754.2016.06.031

Qiu, X. M., Liu, Y. R., and Fu, Q. (2005). *Sequence stratigraphy and sedimentary evolution of the Upper Cretaceous and third systems in subei basin*. Beijing: Geological Publishing House, 1–59.

Sonnenberg, S. A., and Pramudito, A. (2009). Petroleum geology of the giant elm coulee field, williston basin. *AAPG Bull.* 93 (9), 1127–1153. doi:10.1306/05280909006

U.S. Energy Information Administration (2016). *Lower 48 states shale plays*. Washington D C: U.S. Energy Information Administration.

Wang, Z. L. (2013). Research progress, existing problem and development trend of tight rock oil. *Petroleum Geol. and Exp.* 35 (6), 587–596. doi:10.11781/sysydz201306587

Wang, H. F. (2016). Recognition of effective fractures within the oil shale in the fourth member of funing formation in northern Jiangsu basin. *J. Southwest Petroleum Univ. Sci. and Technol. Ed.* 38 (3), 21–27. doi:10.11885/j.issn.1674-5086.2014.08.27.02

Wang, H. W., and Duan, H. L. (2016). Formation condition and enrichment rule of shale oil in the second member of funing formation in yancheng sag. *Complex Hydrocarb. Reserboirs* 9 (3), 14–19. doi:10.16181/j.cnki.fzyqc.2016.03.004

Wang, S. Q., Sun, X. M., and Du, J. Y. (2012). Analysis of structural styles in northern segment of tancheng—lujiang fault zone. *Geol. Rev.* 58 (3), 414–425. doi:10.16509/j.georeview.2012.03.007

Wang, X., Zhang, J. F., and Jiang, W. L. (2016). Transverse structures features of different depths derived from bouguer gravity anomalies in the southern segment of tan-lu fault zone. *Seismol. Geol.* 38 (2), 370–385.

Wang, R., He, W. J., and Zhao, X. M. (2022). Geological section analysis of shale oil in lucaogou formation of well-Ji-174, junggar basin. *Reserv. Eval. Ddvelopment* 12 (1), 192–203. doi:10.13809/j.cnki.cn32-1825/te.2022.01.017

Wang, Z. Q., Fan, Z., and Chen, X. (2023). Global oil and gas development in 2022: situation, trend and enlightenment. *Petroleum Explor. Dev.* 50 (5), 1016–1031. doi:10.1016/S1876-3804(23)60456-2

Wu, S. T., Zhu, R. K., and Luo, Z. (2022). Laminar structure of typical Continental shales and reservoir quality evaluation in central-western basins in China. *China Pet. Explor.* 27 (5), 62–72. doi:10.3969/j.issn.1672-7703.2022.05.006

Wu, Y. Q., Jiang, F. J., Hu, T., Xu, Y., Guo, J., Xu, T., et al. (2024). Shale oil content evaluation and sweet spot prediction based on convolutional neural network. *Mar. Petroleum Geol.* 167, 106997. doi:10.1016/j.marpetgeo.2024.106997

Wu, Y. Q., Hu, T., Jiang, F. J., Guo, J., Wang, F., Qi, Z., et al. (2025a). Lacustrine records of Paleocene-Eocene thermal maximum (PETM) triggered by volcanic activity. *Org. Geochem.* 200, 104899. doi:10.1016/j.orggeochem.2024.104899

Wu, Y. Q., Jiang, F. J., Xu, Y. L., Guo, J., Xu, T., Hu, T., et al. (2025b). Middle Eocene climatic optimum drove palaeoenvironmental fluctuations and organic matter enrichment in lacustrine facies of the Bohai Bay basin, China. *Palaeogeogr. Palaeoclimatol. Palaeoecol.* 659, 112665. doi:10.1016/j.palaeo.2024.112665

Xiong, S. C., Chu, S. S., and Pi, S. H. (2017). Micro-pore characteristics and recoverability of shale oil reservoirs. *Earth Sci.* 42 (8), 1379–1385. doi:10.3799/dqkx.2017.550

Yan, L., Ran, Q. Q., and Gao, Y. (2017). Shale oil occurrence form and recoverability evaluation of shale oil reservoir in lucaogou formation of Xinjiang. *Reserv. Eval. Dev.* 7 (6), 20–26. doi:10.13809/j.cnki.cn32-1825/te.2017.06.004

Yang, H., Li, S. X., and Liu, X. Y. (2013). Characteristics and resource prospects of shale oil and shale oil in ordos basin. *Acta Pet. Sin.* 34 (1), 1–11. doi:10.7623/syxb201301001

Yun, L., He, X. P., and Hua, C. X. (2023). Accumulation characteristics and resource potential of Paleogene Continental shale oil in qintong sag of subei basin. *Acta Pet. Sin.* 44 (1), 174–187. doi:10.7623/syxb202301011

Zan, L., Luo, W. F., and Ma, X. D. (2016). Hydrocarbon generation potential and genetic environments of second member of funing formation in qintong Sag,Subei basin. *Unconv. Oil and Gas* 3 (3), 1–8.

Zhang, X. L., Zhu, X. M., and Zhoug, D. K. (2004). The character of sequence framework of tertiary and Upper Cretaceous in gaoyou sag,subei basin. *Acta Sedimentol. Sin.* 22 (3), 393–399. doi:10.14027/j.cnki.cjxb.2004.03.004

Zhang, J. D., Yang, C. C., and Liu, C. Z. (2010). The deep structures of strike-slip and extension faults and their composite relationship in the southern of tanlu fault zone. *Chin. J. Geophys.* 53 (4), 864–873. doi:10.3969/j.issn.0001-5733.2010.04.011

Zhang, L. Y., Bao, Y. S., Li, J. Y., Li, Z., Zhu, R., and Zhang, J. (2014). Movability of lacustrine shale oil:a case study of dongying Sag,Jiyang Depression,Bohai Bay basin. *Petroleum Explor. Dev.* 41 (6), 703–711. doi:10.1016/s1876-3804(14)60084-7

Zheng, K. F., and Peng, X. L. (2013). Hydrocarbon accumulation and favorable zone of shale oil and gas in Upper Cretaceous Neogene of north Jiangsu basin. *Jiangsu Geol.* 37 (1), 147–154. doi:10.14027/j.cnki.cjxb.2004.03.004

Zhou, S. W., Xue, H. Q., and Guo, W. (2014). Experimenta1 of movable fluid of shale oil reservoir in Jurassic shale oil reservoirs in central sichuan basin. *J. Liaoning Tech. Univ. Nat. Sci.* 33 (6), 768–772. doi:10.3969/j.issn.1008-0562.2014.06.010

Zou, C. N., Zhu, R. K., and Bai, B. (2015). Significance,geologic characteristics.resource potential and future challenges of shale oil and shale oil. *Bull. Mineralogy,Petrology Geochem.* 34 (1), 3–17. doi:10.3969/j.issn.1007-2802.2015.01.001